NASA TECHNICAL NOTE

NASA TN D-5542

NASA TN D-5542

PERFORMANCE OF A TURBOALTERNATOR GAS-BEARING SYSTEM AT STEADY-STATE CONDITIONS

by Roman Kruchowy, James C. Wood, and Joseph S. Curreri

Lewis Research Center
Cleveland, Ohio

NATIONAL AERONAUTICS AND SPACE ADMINISTRATION • WASHINGTON, D. C. • NOVEMBER 1969

1. Report No. NASA TN D-5542	2. Government Accession No.	3. Recipient
4. Title and Subtitle PERFORMANCE OF A TURBOALTERNATOR GAS-BEARING SYSTEM AT STEADY-STATE CONDITIONS		5. Report Date November 1969 6. Performing Organization Code
7. Author(s) Roman Kruchowy, James C. Wood, and Joseph S. Curreri		8. Performing Organization Report No. E-5225
9. Performing Organization Name and Address Lewis Research Center National Aeronautics and Space Administration Cleveland, Ohio 44135		10. Work Unit No. 120-27 11. Contract or Grant No.
12. Sponsoring Agency Name and Address National Aeronautics and Space Administration Washington, D.C. 20546		13. Type of Report and Period Covered Technical Note 14. Sponsoring Agency Code

15. Supplementary Notes

16. Abstract

This reports presents the results of experimental testing of the gas-bearing system in a Brayton-cycle turboalternator. The turboalternator was tested under design and off-design steady-state conditions. Pressure ratio across the turboalternator was varied from 1.1 to 1.5, alternator output was varied from 0 to 33 kWe, and liquid-coolant flow was adjusted as appropriate. The gas bearings operated satisfactorily throughout the tests. At high alternator outputs, thrust loads in excess of 200 percent of the design value were produced.

17. Key Words *(Suggested by Author(s))* Gas-bearing performance	18. Distribution Statement Unclassified - unlimited		
19. Security Classif. (of this report) Unclassified	20. Security Classif. (of this page) Unclassified	21. No. of Pages 31	22. Price* $3.00

*For sale by the Clearinghouse for Federal Scientific and Technical Information Springfield, Virginia 22151

PERFORMANCE OF A TURBOALTERNATOR GAS-BEARING SYSTEM AT STEADY-STATE CONDITIONS

by Roman Kruchowy, James C. Wood, and Joseph S. Curreri

Lewis Research Center

SUMMARY

The results of experimental operation of the gas-bearing - rotor system in a turboalternator under various steady-state conditions are presented in this report. Pressure ratio across the turboalternator was varied from 1.1 to 1.5; alternator output was varied from 0 to 33 kilowatts electric; and liquid-coolant flow was adjusted as appropriate. At high alternator outputs, thrust loads in excess of 200 percent of the design value were produced.

Operation of the bearing-rotor system was found to be stable under all load conditions. Magnetic excitation of the bearing-rotor system was negligibly small, and there was no noticeable effect of high-order magnetic harmonics on bearing stability.

The bearing-rotor system passed through critical speeds without excessive vibration. The vibrational amplitudes of the rotor relative to the bearing pads at the critical speeds were negligible and of no practical concern. No bearing contact was detected, other than the normal intermittent contact for approximately 3 seconds during the startup and shutdown periods.

It was found that total reduction of the oil coolant flow to the heat exchangers and support ring of the anti-drive-end bearing is possible under normal vertical operating conditions. Partial reduction of oil coolant flow to the drive-end-bearing heat exchangers was achieved.

Study of pad-motion oscilloscope photographs revealed no apparent effects of bearing-pivot wear. However, the turboalternator was not disassembled for inspection of the pivots.

INTRODUCTION

In order to expand NASA's mission capabilities in space, the Lewis Research Center

is now investigating several dynamic power systems. One system under consideration operates on the Brayton cycle and uses argon as the working fluid. As part of this system, a turbine-driven alternator (turboalternator) was built to provide electrical power.

The turboalternator design criteria included high efficiency and long life. Because of these criteria, gas-lubricated bearings were chosen over conventional bearings to support the shaft. The need for an oil-lubrication system and possible contamination of the system working fluid were thereby eliminated. Self-acting (hydrodynamic) bearings were chosen for simplicity over externally pressurized (hydrostatic) bearings.

Self-acting gas bearings supporting the shafts of turbine-driven compressors are reported in references 1 and 2. One of the unknowns in gas bearings for turboalternators not found in the turbocompressor is the effect of the magnetic forces on the bearing-rotor system. Other problems common to all gas bearings are the maintenance of small shaft-bearing clearances and the reduction of rotor vibration to a minimum in order to operate within the low damping capabilities of gas bearings.

A bearing-rotor simulator containing an alternator was built during the design phase of the turboalternator in order to determine the bearing-rotor system characteristics. The simulator was operated to an output of 12 kilowatts electric in order to check the effects of the magnetic forces. It also had provisions for changing the bearing clearance, as would result from temperature effects. The simulator performance using gas bearings of the same design used in the turboalternator is covered in reference 3.

The contractor performed acceptance tests with the turboalternator axis inclined at 45° to the vertical; thus, gravity affected both journal- and thrust-bearing loads (ref. 4). In the tests conducted at Lewis the turboalternator axis was held vertical. This procedure more closely simulated space conditions by eliminating gravitational forces from the journal bearings. The contractor tests were also limited to a brief checkout using air and turbine inlet temperatures to 200° F (366 K). Thorough testing using argon at elevated temperatures was performed at Lewis. Special consideration was given to evaluation of the gas bearings under various electrical power conditions, steady state as well as transient. This report contains the results of the steady-state testing done on the gas bearings.

APPARATUS

Turboalternator Description

The turboalternator consists of a four-pole homopolar inductor alternator and a two-stage axial-flow turbine mounted on a single shaft. The shaft is supported on two self-acting, tilting-pad journal bearings and an inward-pumping, spiral-groove, self-

acting thrust bearing. The turboalternator is shown in figure 1.

The journal bearings are located between the turbine and alternator and between the alternator and thrust bearing. Each bearing consists of four pads; and each pad covers an 80^{o} arc of the shaft circumference. The pads pivot on a nonconforming ball and socket (pivot ball diameter, 0.625 in. (1.58 cm); socket diameter, 0.812 in. (2.06 cm)). The pivot ball is mounted to the bearing housing by a flexible beam (flexure). The flexure allows for some dynamic movement of the pad and a limited amount of thermal growth. The bearing parts are shown in figure 2.

The heat generated in the journal bearings is removed by heat-exchanger sleeves located around the shaft on each side of the bearings. The heat is conducted from the shaft to the heat exchangers through a 0.005-inch (1.27×10^{-2}-cm) radial gap. The inner surface of the shaft under the journal-bearing area is plated with a 0.125-inch- (0.318-cm-) thick layer of copper. The plating is used to maintain uniform temperatures along the shaft under the bearing pads. A schematic drawing of the journal bearing and heat exchangers is shown in figure 3.

The support ring, holding the bearing assembly, contains coolant passages to allow for bearing clearance adjustment during operation. Since the temperature of the support ring is largely determined by the coolant temperature, adjustment of coolant temperature results in a bearing clearance adjustment.

A schematic view of the thrust bearing is shown in figure 4. Both the main and reverse thrust bearings can be operated hydrostatically, but only the main thrust bearing can be operated hydrodynamically. The thrust load on the main bearing is 87 pounds (390 N) when the turboalternator is in the vertical position and at a turbine design condition. Of this, 57 pounds (25 kg) is shaft weight and 30 pounds (130 N) is aerodynamic forces. The main thrust bearing is designed for a maximum 250-pound (1100-N) load to provide for transient loads encountered in startup. The main-thrust-bearing stator (fig. 5) is flexibly mounted to permit dynamic alinement of the stator with the thrust runner. Liquid flows through the main thrust stator to cool it. Details of thrust-bearing design are presented in reference 3.

A small amount of argon is fed through the turboalternator from the thrust-bearing end of the machine. The gas flows through and around the shaft toward the turbine end (fig. 6). The gas then enters the main gas flow through gap passages before and after the turbine. The purpose of the gas is to prevent backflow of hot turbine gas into the bearing area and to assist in heat removal. The cooling argon was obtained from a source external to the closed loop, as shown in the schematic diagram of figure 7. In a space power system, this gas supply would be bled from the discharge of the argon-circulating compressor.

Test Facility Description

The test facility to operate the turboalternator (fig. 7) is described in detail in reference 5.

The argon supplied to the turbine was heated by the electric heater. Inlet pressure was controlled by regulating the flow through the turbine bypass. Turbine weight flow was measured by the venturi upstream of the turboalternator, and pressure ratio was controlled by the valve at the turbine discharge. This control valve was also used to control turbine speed for some of the tests.

The oil loop supplied coolant to the alternator-stator heat exchangers and to the bearing support ring at each of the bearings. Coolant temperatures and the oil flow rates to the alternator, bearing heat exchangers, and support rings could be controlled individually.

The electrical output of the alternator was absorbed by load banks. A voltage-regulator-exciter supplied the current to the alternator field needed to maintain required alternator output voltage. Tests were conducted with balanced and unbalanced alternator loads at varying power factors, as well as with step load transients.

Instrument Description

Chromel-Alumel thermocouples were used to measure turboalternator internal temperatures and turbine inlet and outlet gas temperatures. The inlet and outlet gas temperatures were measured with bare spike stream thermocouples mounted on rakes. The oil coolant temperatures were measured with iron-constantan thermocouples immersed in the oil stream.

Pressures were measured with strain-gage-type transducers. Static and total pressures were measured at the turbine inlet and outlet. Turboalternator case pressures were also measured.

The turbine weight flow was measured with a calibrated venturi, coolant oil flow with turbine flowmeters, and coolant gas flows with rotameters.

Capacitance probes were employed to measure journal motion relative to the housing, thrust-bearing film thickness, film thickness between each bearing pad and the shaft, and the dynamic motion of the bearing pads relative to the turboalternator housing.

The output of the probe unit is a voltage that is directly proportional to the clearance. All the outputs of the capacitance probe units are recorded on an FM magnetic tape recorder. The outputs of the bearing clearance probes were also sent to oscilloscopes for continuous monitoring. The wattmeters, voltmeters, and ammeters used to measure alternator output were the wide-frequency-range, true-rms electronic type.

Turboalternator shaft speed was measured with three magnetic speed pickups. Six notches were cut in the thrust-bearing runner to activate these speed pickups.

PROCEDURE

The initial steps, before rotation, consisted primarily of (1) establishing rated coolant (Dow-Corning 200) flows and temperature (nominally 200° F (366 K)) into the bearing heat exchangers, (2) adjusting gas coolant flow rate through the turboalternator, and (3) supplying hydrostatic jacking gas to the thrust bearings. Rotation was then initiated by opening the turbine outlet pressure-control valve.

At 12 000 rpm, the thrust-bearing hydrostatic jacking gas was turned off; at this point only the hydrodynamic operating mode existed on all bearings. Coolant flow and temperature to the journal support rings were then adjusted to give an acceptable value of journal-bearing clearance.

Care was taken in all tests to observe the recommended bearing clearances. This includes the journal-bearing clearance range of 0.5 to 1.5 mils (1.3×10^{-3} to 3.8×10^{-3} cm) radial, the main-thrust minimum clearance of 0.8 mil (2.03×10^{-3} cm), and the reverse-thrust minimum clearance of 1.0 mil (2.54×10^{-3} cm). When satisfactory journal-bearing clearances had been established, the main loop heater was turned on.

At approximately 900° F (756 K) turbine inlet gas temperature, the drive-end bearing outer mount ring approached 400° F (478 K), which is the maximum operating temperature of the capacitance probe instrumentation wires, located in the outer mount ring. In order to protect these wires, cooling air was applied. It remained on whenever turbine inlet gas temperature exceeded 900° F (756 K).

Once turbine and coolant design conditions have been established (table I), other

TABLE I. - DESIGN CONDITIONS

Turbine:	
Inlet total temperature, °F (K)	1225 (936)
Inlet total pressure, psia (N/m^2)	8.45 (5.82×10^4)
Pressure ratio, total to static	1.26
Rotative speed, rpm	12 000
Coolant (Dow-Corning 200) flow rates, lb/min (kg/min):	
Drive-end-bearing (forward) heat exchanger	3.6 (1.63)
Drive-end-bearing (rear) heat exchanger	1.5 (0.68)
Anti-drive-end-bearing (forward) heat exchanger	1.7 (0.77)
Anti-drive-end-bearing (rear) heat exchanger	0.4 (0.18)
Thrust-bearing heat exchanger	1.7 (0.77)

pressure ratios and speed conditions were achieved by regulating the outlet pressure-control valve and adjusting the load banks.

For all the tests performed, except the coolant flow reduction experiment, the heat-exchanger flow rates were set at values listed in table I. Coolant flow and temperature to the journal-bearing support rings were adjusted, if necessary, before each test series to obtain an acceptable clearance.

When the turboalternator was shut down, the thrust-bearing hydrostatic jacking gas was again turned on before turbine gas flow was stopped. Journal-bearing rubbing at low shaft speeds was minimized by manually exciting the alternator field. This caused the alternator to act as a brake.

DISCUSSION OF RESULTS

The major objective, to run the turboalternator at design conditions, was met by running it at design inlet temperature of 1225^{o} F (936 K) continuously for 100 hours. The turboalternator was further run to evaluate its design and endurance; the total operating time was 1165 hours, during which it was started and stopped 24 times.

In addition to the design-condition testing, various off-design conditions were tested by varying (1) turbine inlet temperature from 400^{o} to 1225^{o} F (478 to 936 K), (2) pressure ratio from 1.1 to 1.5, (3) alternator output from 0 to 33 kilowatts electric, (4) power factor from 0.6 lagging to 1.0, (5) coolant flow to the heat exchangers and support ring, and (6) rotative speed from 7000 to 14 400 rpm. Also included were single-phase and multiphase short circuits.

Starting and Stopping

When rotation started, the journals would rub intermittently for about 3 seconds until full hydrodynamic operation was obtained at approximately 2000 rpm. During the 1165-hour test involving a total of 24 starts and stops, the journal rubbing was observed to have no effect on bearing performance.

As the turbine temperature approached design conditions, the drive-end-bearing clearance changed by thermal expansion of both the shaft and the bearing-mount ring. The anti-drive-end-bearing clearance change was negligible. Figure 8 shows the radial clearance as changed by turbine inlet temperature. Even though the change in clearance of the front bearing was large, it should be noted that it still remained within the design range of 0.5 to 1.5 mils (1.3×10^{-3} to 3.8×10^{-3} cm).

The dip in the curve of the drive-end-bearing clearance was caused by cooling air

applied to the drive-end-bearing mount ring. The cooling air prevented the mount ring, to which the capacitance-probe instrumentation wire was connected, from exceeding the maximum wire operating temperature.

Effect of Alternator Output on Journal Orbits and Bearing Clearances

In figure 9 the variation of bearing clearance with alternator output at three speeds (10 000, 12 000, and 14 400 rpm) is shown. At a given speed and turbine inlet temperature, the drive-end-bearing clearance is more sensitive to alternator output than is the anti-drive-end clearance. This is a result of turbine exhaust conditions; that is, high power levels result in reduced turbine exhaust temperatures. This affects the drive-end-bearing supports and results in an acceptable drop in clearance.

The reduction of clearance with increase in rotational speed is primarily due to a combination of centrifugal and thermal shaft growth.

The probable reasons for shaft temperature rise are the bearing frictional losses (proportional to the square of the shaft speed), and the reduction in bearing gas coolant flow at higher speeds. This reduction in bearing gas coolant flow was an inherent property of the system and could not be traced to any specific cause.

Orbit traces (motion of shaft center) are presented in figures 10 and 11 to show orbit size; the location of the orbit trace on the oscilloscope is not significant. Figure 10 shows the orbit diameter variation with output power and at a fixed speed of 12 000 rpm. Figure 11 shows the orbit diameter variation at 10 000, 12 000, and 14 400 rpm and at a fixed pressure ratio of 1.26. In both cases the orbit diameter remained virtually the same and gave no indication of impending dangerous conditions.

Effect of Alternator Output on Bearing-Pad Motion

The locations of the capacitance probes and the bearing-pad pivot point are shown in figure 12. Both the roll and film thickness probes are located within the bearing pad; the pitch probe is fastened directly above the pad surface.

The pitch and roll probes were used to show only the oscillatory movement; the film trace shows both the oscillatory movement and the film thickness.

The test program included evaluation of bearing-pad dynamics at various load conditions. The tests included power outputs from 0 to 33 kilowatts electric and short circuits, in order to determine the effect of unbalanced magnetic force on the bearing system. The unbalanced magnetic force (due to rotor eccentricity) rotates predominantly at twice the frequency of the shaft rotation. This produces a two-per-revolution ex-

citation. However, during short circuits higher frequencies can be achieved. This may produce forces with frequency components close to resonance of either the rotor or the pads of the journal bearing, thus exciting large vibrational amplitudes that may lead to failure. This is especially true of higher rotor vibrational frequencies, at which the bearings lose most of their damping capability. Therefore, it was necessary to investigate bearing performance at electrical load conditions beyond a design operating condition.

Under all load levels from 0 to 33 kilowatts electric and also short circuits, the movements of the pads remained virtually unchanged. Typical examples of what appear to be bearing-pad two-per-revolution motions in the pitch direction are shown in figure 13. There is no substantial amplitude variation with output power to cause detrimental operation.

A small amount of pad roll about the pivot was detected at high alternator current output. Roll and film thickness traces were examined during a three-phase short-circuit test, one of the more severe conditions. The roll-probe trace during the short circuit indicated an increase in clearance; the film trace, however, indicated a decrease in clearance. Since the film and roll probes are mounted on opposite sides of the pivot, this would indicate the pad rolling about the roll axis. The probable cause of this rolling is an increase, during the short circuit, in end-turn magnetic-flux leakage interacting with the pad material. The end of the pad nearest the alternator is affected to a greater degree, thereby causing a dip in that end. The clearance reduction, however, is negligible and does not give cause for concern.

Rotor-Bearing Resonance Effects

Several tests were made by varying the speed of the turboalternator in the 6000- to 10 000-rpm range in an attempt to excite the rotor-bearing criticals. Three criticals were encountered at approximately 7200, 8000, and 9600 rpm. At all three points, the vibrational amplitudes were insignificantly small. The 7200- and 9600-rpm criticals are close to the predicted rigid-body resonances of the rotor. The disturbance occurring at 8000 rpm could be the result of turbine-stator wakes (ref. 4).

Figure 14 is an example of the anti-drive-end shaft orbit at the 7200- and 9600-rpm resonant points. An insignificant increase in the orbit diameter is found at the design operating condition of 12 000 rpm (see fig. 11). A similar insignificant increase in orbit diameter exists at the drive end.

The variation of film thickness between the pads and the rotor at a resonant speed (7200 rpm) is shown in figure 15(a). To serve as a comparison, the film thickness oscillation at the design speed (12 000 rpm) is included. These are typical examples of

film thickness variation at resonance and design conditions. The peak-to-peak variation of the film thickness is 0.15 mil (0.38×10^{-3} cm) at resonance. This movement is small compared to the nominal film thickness of 1.0 mil (2.54×10^{-3} cm); therefore, the possibility of shaft rub is not present.

A similar situation exists in the reverse-thrust-bearing film thickness shown in figure 15(b). At resonance the nominal clearance is 1.0 mil (2.54×10^{-3} cm); therefore, the 0.2 mil (0.51×10^{-3} cm) peak-to-peak variation is far removed from possible stator-to-runner contact.

In conclusion, these results indicate that the rotor-bearing system is stable from startup to 12 000 rpm.

Effects of Varying Power Factor

Figure 16 shows the effect of varying power factor on clearance at a constant output power and speed. The bearing-pad temperature (which is nearly the same as shaft temperature) and support temperature are also plotted. The major cause of clearance change is the pad (or shaft) temperature increase which results with decrease of power factor. At low power factors, a lagging armature current produces a demagnetizing effect in the alternator which has to be compensated by increasing field current in order to maintain a constant power output. As a result, increased armature copper losses, field copper losses, and stray load losses generate heat and increase pad (or shaft) temperature.

Influence of Varying Coolant Oil Flow Rate To Heat Exchangers and Support Rings

This test was designed to show the effects of variations of oil flow rate on journal-bearing clearance. The data were also used to show the relation of bearing-pad temperature and pressure as a function of bearing clearance. A separate test was conducted for each journal. Both tests were conducted by first establishing design conditions and then making increment changes only to the oil flow rate of the heat exchangers of the journal under test. All other parameters were kept as constant as possible. No adjustments were made to loop operations once each test had begun. Flow to the support ring was not adjusted until total reduction of flow to the heat exchangers was achieved.

The drive-end bearing clearance as a function of its heat-exchanger oil flow rate is shown in figure 17. The oil flow rate is expressed in percent of the design flow rate. The clearance is the average clearance of the four pads. The results show the bearing clearance decreasing with decreasing heat-exchanger oil flow rate. The decrease in

heat-exchanger oil flow rate raises the temperature of the rotating shaft. This causes the shaft diameter to expand, thereby decreasing bearing clearance.

Further reduction of coolant flow was not attempted because the clearance became extremely sensitive to coolant flow rate; that is, a slight decrease in coolant flow was followed by a rapid decrease in clearance.

A similar test was conducted on the anti-drive-end bearing. In this case, however, coolant flow to the heat exchangers was reduced to zero. A 0.2-mil (0.51×10^{-3} cm) reduction in clearance resulted. Afterward, the coolant flow to the support ring was turned off and the bearing clearance was subsequently increased to 1.35 mils (3.43×10^{-3} cm). This clearance level falls within the allowable limits of 0.5 to 1.5 mils (1.3×10^{-3} to 3.8×10^{-3} cm). This test indicates that no coolant oil is required to the heat exchangers and support ring of the anti-drive-end bearing at design, vertical (0-g) operating conditions. The effect of zero coolant flow to the heat exchangers and support rings has not been determined for a startup condition.

Pad Temperature and Pressure

Figures 18 and 19 show how the average bearing-pad temperature and pad-pivot-point pressure varied with bearing clearance in the drive-end journal during the oil flow reduction tests. As previously mentioned the reduction in clearance is due to the increase in pad (or shaft) temperatures. The pad temperatures did not reach the design values, as noted in reference 5.

The pad pivot pressure plotted in figure 19 is the hydrodynamic pressure rise generated in the bearing. The pressure is the difference between bearing cavity pressure and the bearing pressure measured at the hydrostatic gas ports. The bearing cavity pressure was maintained constant at 6.36 psia (4.39×10^{4} N/m^2) throughout the test. As expected, the pressure dropped as the clearance increased.

Thrust-Bearing Performance

The effect of turbine pressure ratio (at a constant inlet pressure) on the load applied to the main thrust bearing is presented in figure 20. This thrust load is due primarily to a combination of shaft weight, aerodynamic thrust forces, and turboalternator cavity pressure differentials.

The thrust load value was determined by using a capacitance probe to monitor the stator deflection in the axial direction (see fig. 4). An initial deflection was obtained with the shaft resting on the stator. This deflection represented the shaft weight only. From this point any other deflection can be converted to a thrust load value by multiplying

by the known stiffness of the stator flexure supports. Obtaining a consistent and repeatable initial deflection was not achieved. Therefore, a variation of ±5 pounds (±22.2 N) in calculated thrust load values exists.

The variation of thrust load and clearance is shown in figure 21 for three speeds: 10 000, 12 000, and 14 400 rpm. At the turbine design conditions and a load of 84 pounds (387 N), a very satisfactory film thickness of 1.55 mils (3.94×10^{-3} cm) was obtained. This is considerably greater than the allowable main-thrust-bearing minimum clearance of 0.8 mil (2.03×10^{-3} cm).

It can be seen that good clearances are obtained for a large range of pressure ratios. For example, at a pressure ratio of 1.4, which corresponds to a nominal power output level of 14 kilowatts electric (~60 percent above design), the thrust load is 100 pounds (445 N) (fig. 20). At this thrust load a clearance of 1.4 mils (3.56×10^{-3} cm) is still maintained. At a 33-kilowatt-electric power output level, with the thrust load over 200 percent of the design value, the clearance was reduced to 1.1 mils (2.79×10^{-3} cm). This clearance, however, is still above the allowable minimum.

Figure 22 presents oscilloscope traces which indicate the behavior of the main- and reverse-thrust bearings at three load conditions at 12 000 rpm. Increasing loads are associated with an increase in pressure ratio. The traces indicate there is no significant change in the dynamic response with increased thrust load.

Long-Term Operation

In an effort to determine the effect of wear on the pad pivots, photographs were taken of the roll and pitch motions at 200 and 1100 hours of operation. The pivot configuration consisted of M-1 tool steel against M-1 tool steel. In addition, an electrofilm coating on the components was used to inhibit corrosion of the pivot contact zone. Figure 23 indicates that little change in motion occurred in either bearing. (The roll motion was not recorded at the 1100-hr point because of instrumentation failure.)

No further effect of long-term operation can be definitely established until the turboalternator is disassembled for inspection.

SUMMARY OF RESULTS

The turboalternator gas-bearing system was tested at various load conditions (0 to 33 kWe), speeds from startup to 14 400 rpm, and various heat-exchanger flow rates. The results of these tests are summarized as follows:

1. No condition of actual or imminent bearing contact or instability was detected,

other than the normal intermittent contact of the journals with the pads for approximately 3 seconds during the period of startup and shutdown. The rubbing that did occur was observed to have no effect on bearing performance for the 1165 hours of operation and the 24 start-stop cycles.

2. The shaft-orbit diameter at all load conditions remained virtually unchanged. Varying the speed from 10 000 to 14 400 rpm also resulted in no appreciable orbit-size variation. The orbit diameters at the system criticals were also small enough to be of no concern.

3. Magnetic excitation of the bearing system was negligibly small. The two-per-revolution motion in the pitch direction was too insignificant to be of practical concern even during short-circuit testing. There was no noticeable effect of high-order magnetic frequencies on bearing stability. The bearing pads were observed to roll when high-current tests were performed, but to no significant amount.

4. The thrust bearing demonstrated good stability at various load conditions. The thrust-bearing film thickness variation even at the system criticals (7200 and 9600 rpm) was small enough to be of no practical consequence.

5. Thrust-bearing clearances remained above the minimum limits even under large thrust loads at high power levels. At an output of 33 kilowatts electric, the thrust load was above 200 percent of the design value but a satisfactory clearance was observed.

6. Total reduction of oil coolant flow to the anti-drive-end heat exchangers and support ring was possible under design operating condition (vertical shaft, and 9-kWe alternator output). Oil coolant flow to the drive-end bearing was reduced to 30 percent of design; further reduction could not be obtained because of increased clearance sensitivity to oil coolant flow rate.

7. Study of pad-motion oscilloscope photographs revealed no apparent effect of bearing-pivot wear. However, the turboalternator was not disassembled for inspection of the pivots.

Lewis Research Center,
National Aeronautics and Space Administration,
Cleveland, Ohio, September 2, 1969,
120-27.

REFERENCES

1. Grassam, N. S.; and Powell, J. W., eds.: Gas Lubricated Bearings. Butterworths, Inc., 1964.

2. Sternlicht, B.: Gas-Bearing Turbomachinery. Paper 68-LUBS-32, ASME, June 1968.

3. Frost, A.; Lund, J. W.; and Curwen, P. W.: High-Performance Turboalternator and Associated Hardware. II - Design of Gas Bearings. NASA CR-1291, 1969.

4. Cohen, R.; Gilroy, W. K.; and Spencer, W. B.: High-Performance Turboalternator and Associated Hardware. I - Design of Turboalternator. NASA CR-1290, 1969.

5. Wood, James C.; et al.: Preliminary Performance Characteristics of a Gas-Bearing Turboalternator. NASA TM X-1820, 1969.

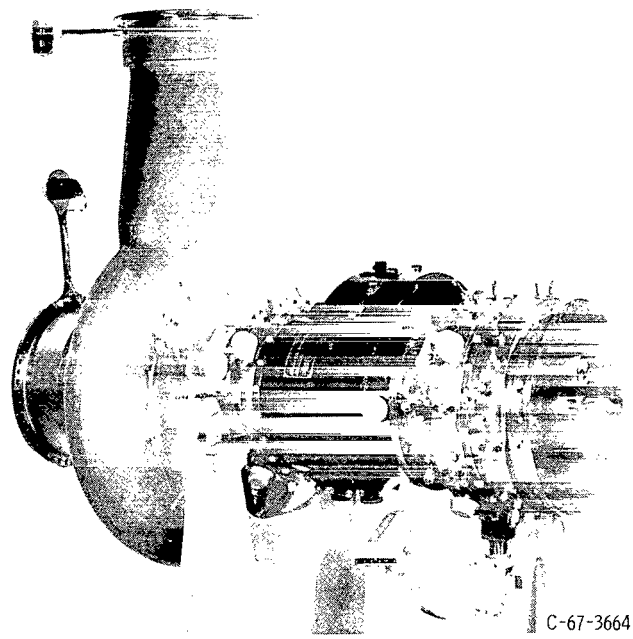

Figure 1. - Turboalternator.

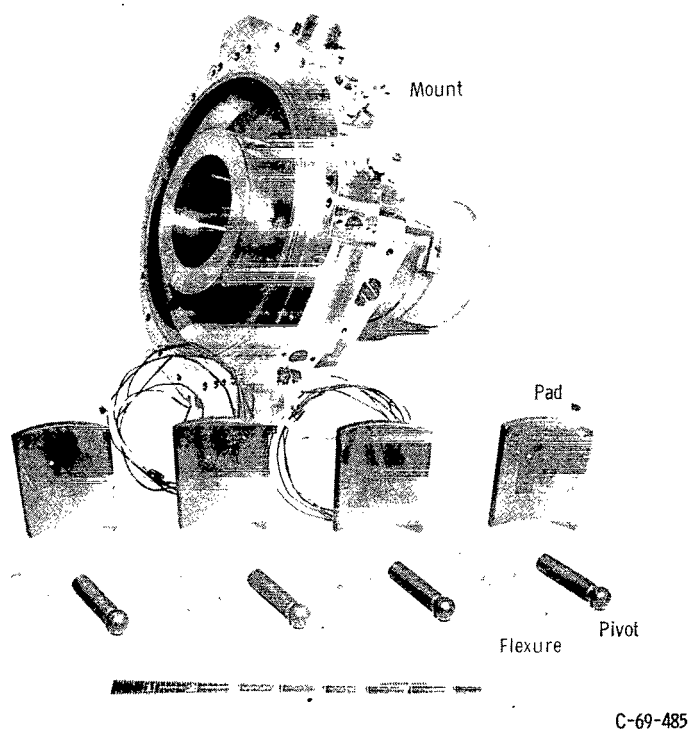

Figure 2. - Parts layout for front journal-bearing assembly.

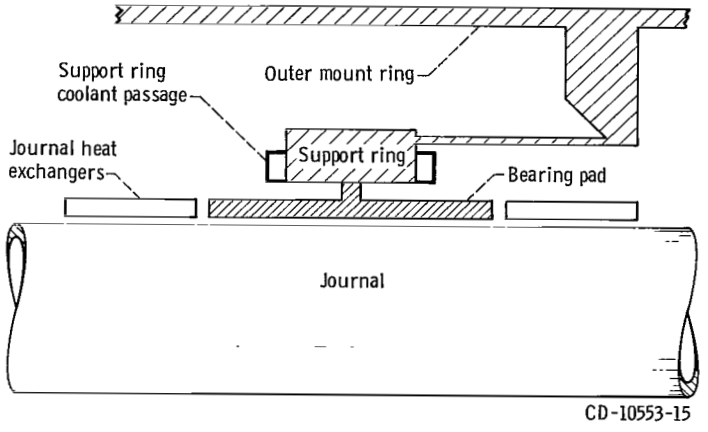

Figure 3. - Schematic drawing of journal bearing.

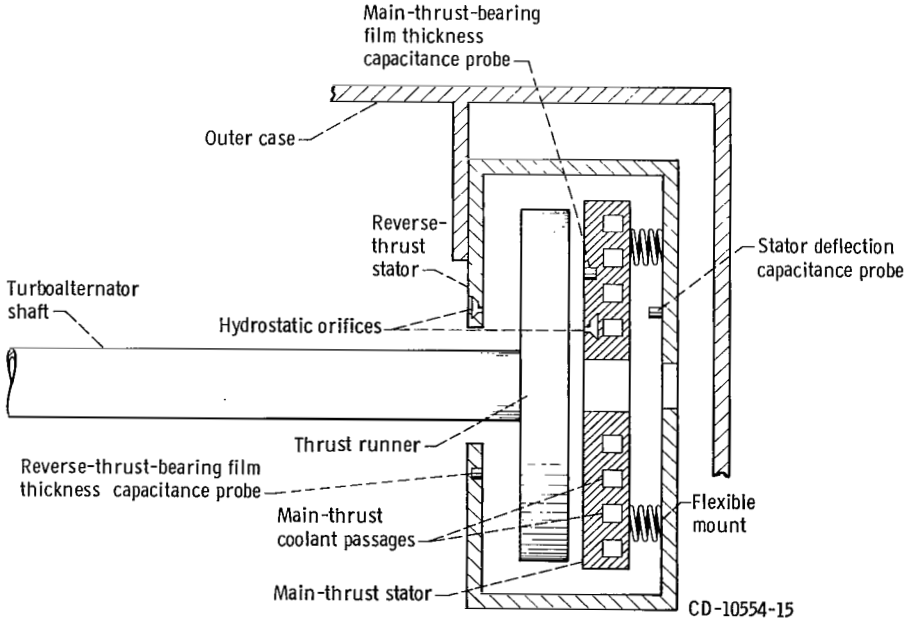

Figure 4. - Schematic drawing of thrust bearing.

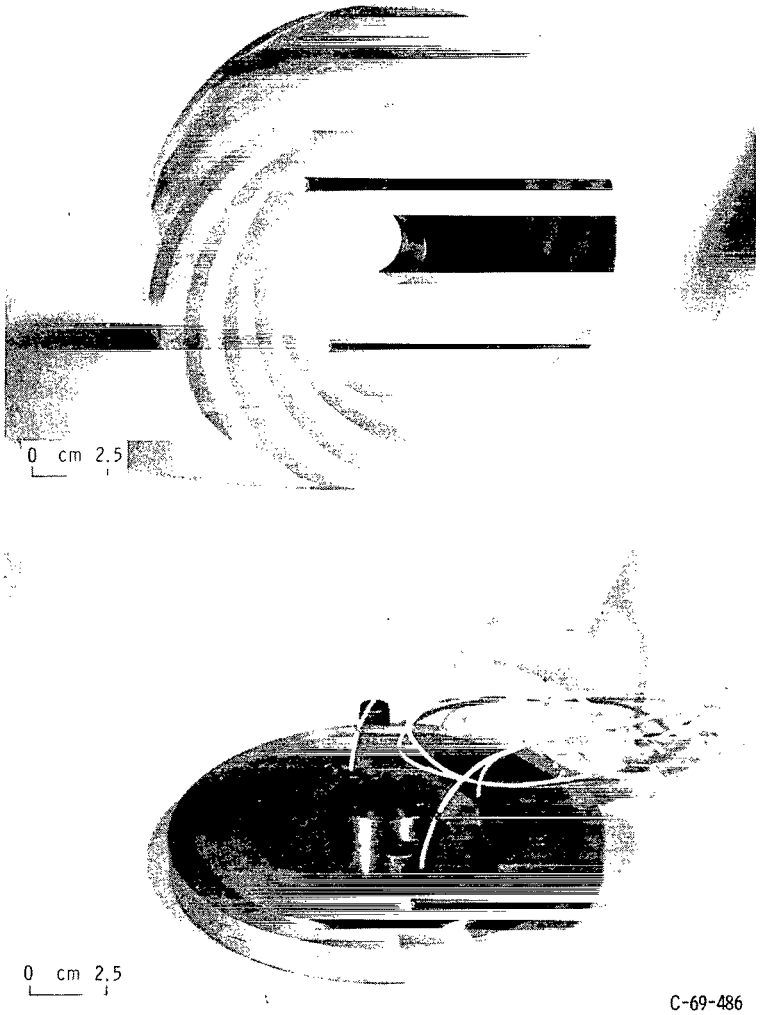

Figure 5. - Main-thrust-bearing stator.

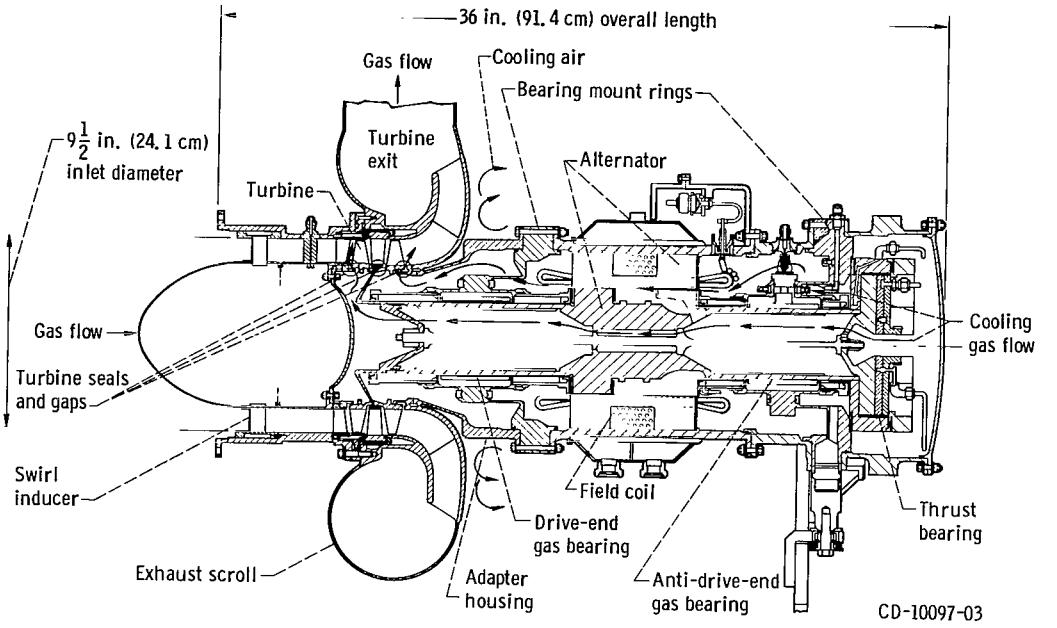

Figure 6. - Cross-sectional view of turboalternator.

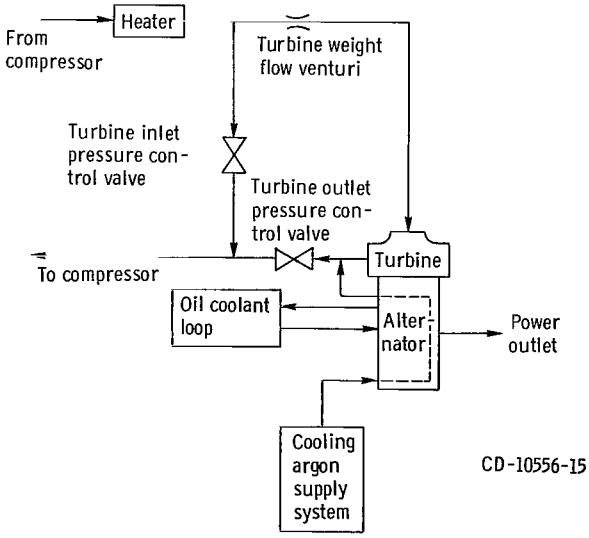

Figure 7. - Schematic drawing of Brayton-cycle turboalternator test facility.

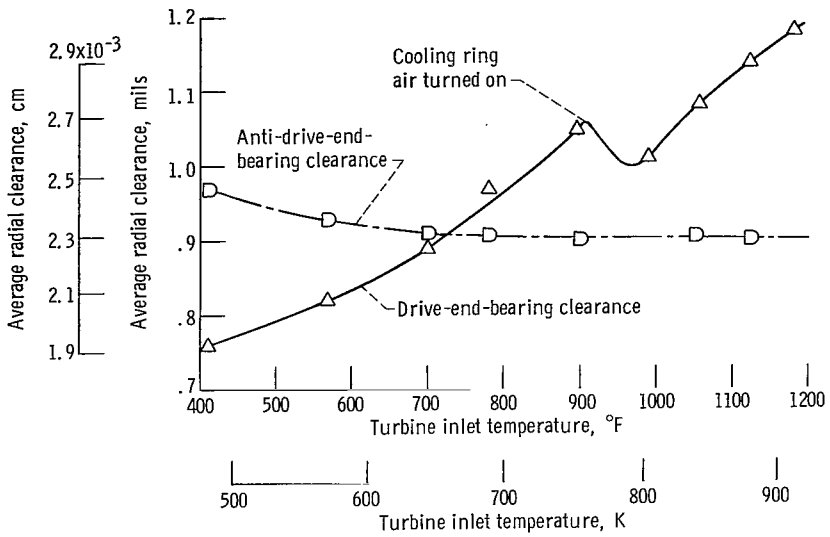

Figure 8. - Effect of turbine inlet temperature on journal clearances. Turbine inlet pressure, 8.45 psia (5.82 N/cm^2); pressure ratio, 1.26; speed, 12 000 rpm.

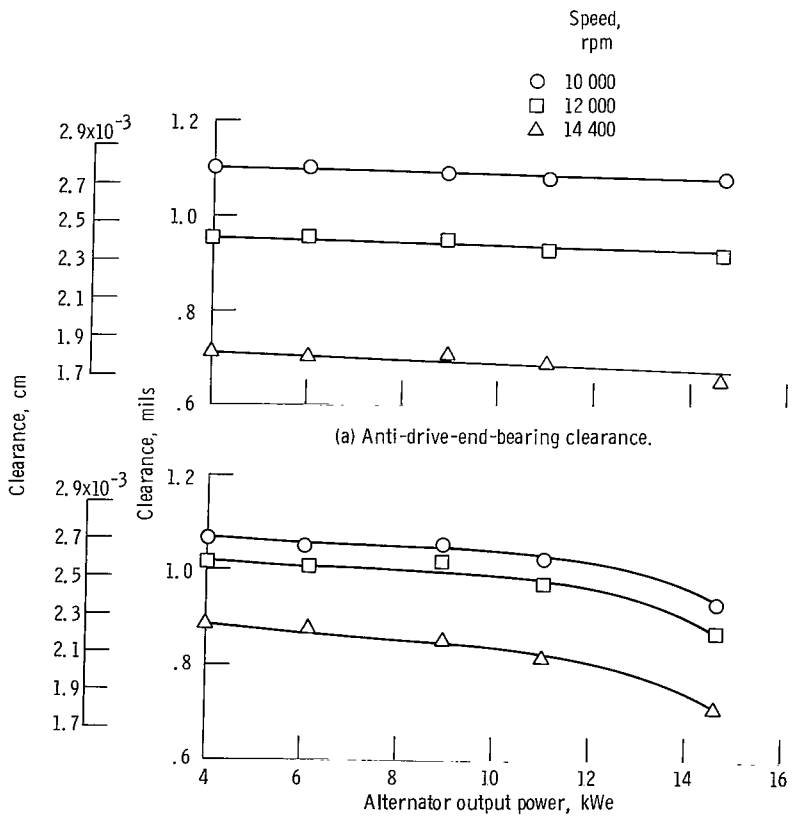

(a) Anti-drive-end-bearing clearance.

(b) Drive-end-bearing clearance.

Figure 9. - Variation of bearing clearance with alternator output at three speeds. Turbine inlet pressure; 8.45 psia (5.82 N/cm^2); turbine inlet temperature, 1225° F (936 K).

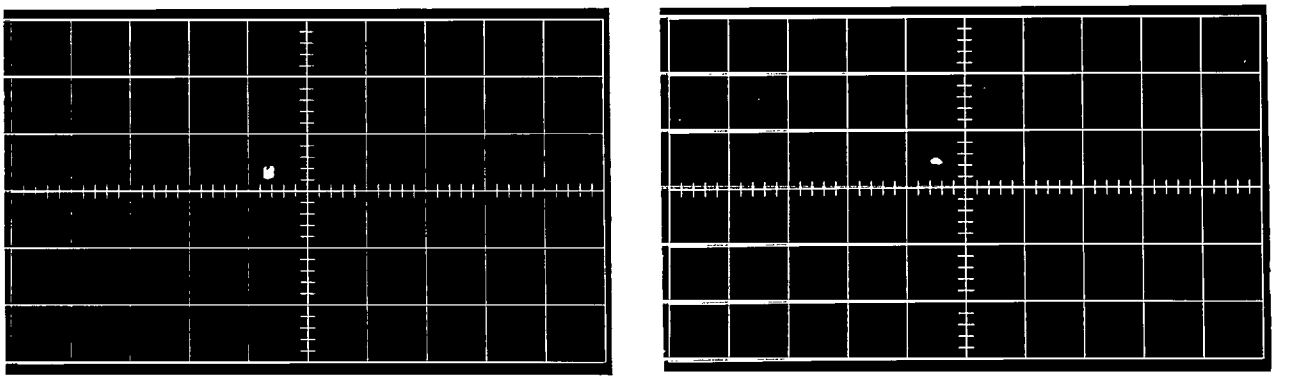

(a) Alternator output, 0 kilowatt electric.

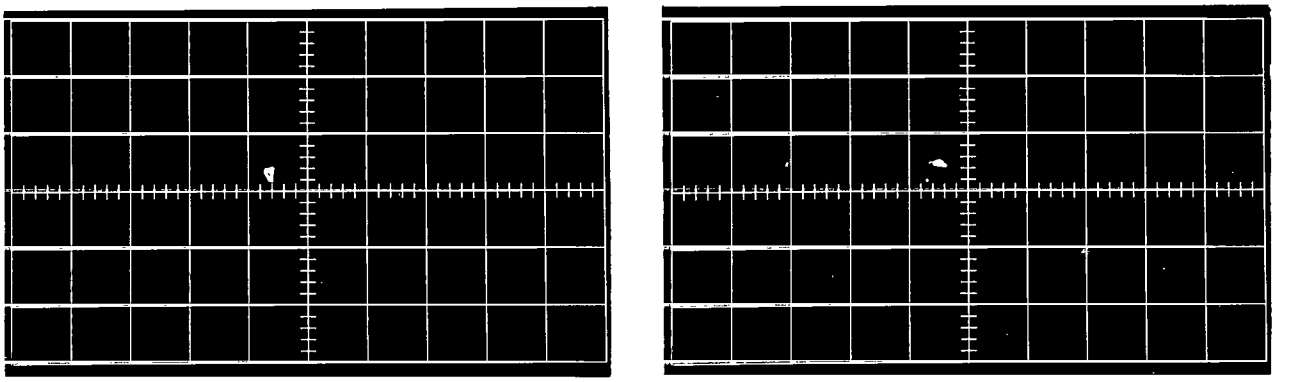

(b) Alternator output, 9 kilowatts electric.

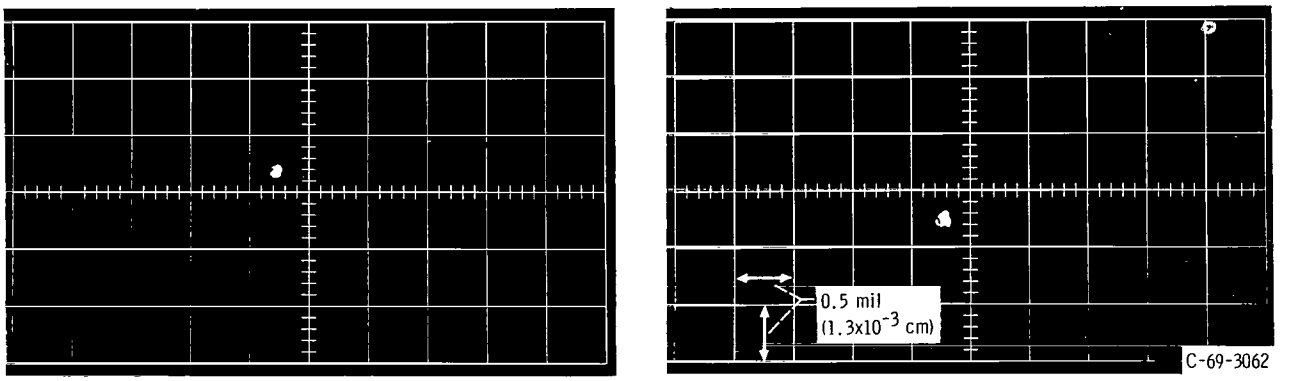

Drive-end journal orbit

Anti-drive-end journal orbit

(c) Alternator output, 33 kilowatts electric.

Figure 10. - Journal-orbit diameters at various alternator outputs. Turbine inlet pressure, 8.45 psia (5.82 N/cm^2); turbine inlet temperature, 1225° F (936 K); alternator speed, 12 000 rpm.

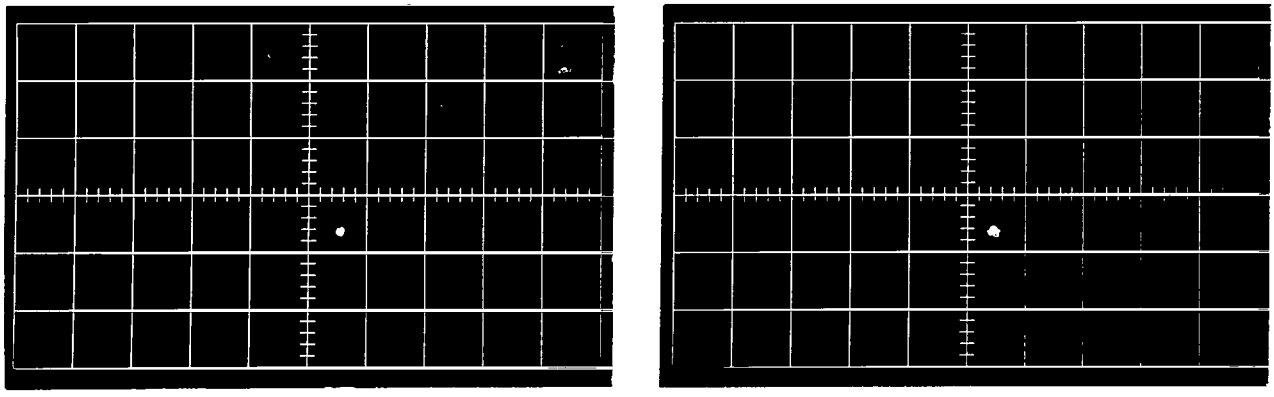

(a) Alternator speed, 14 400 rpm.

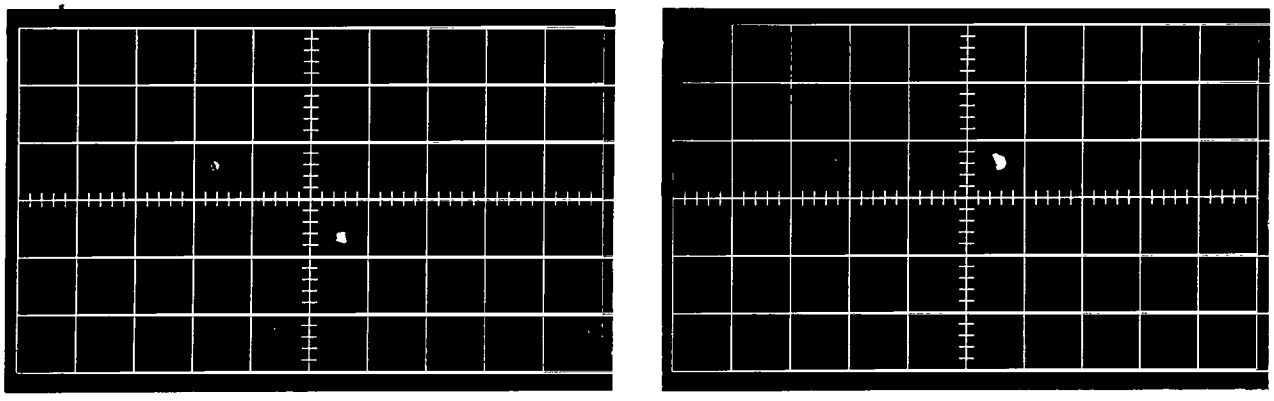

(b) Alternator speed, 12 000 rpm.

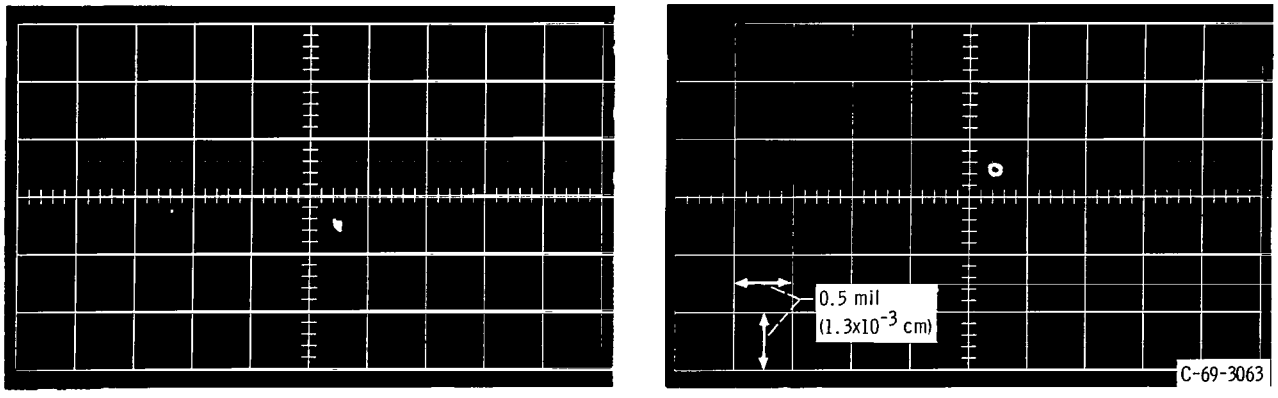

Drive-end journal orbit

Anti-drive-end journal orbit

(c) Alternator speed, 10 000 rpm.

Figure 11. - Journal-orbit diameters at underspeed, design, and overspeed conditions. Turbine inlet pressure, 8.45 psia (5.82 N/cm^2); turbine inlet temperature, 1225° F (936 K); pressure ratio, 1.26.

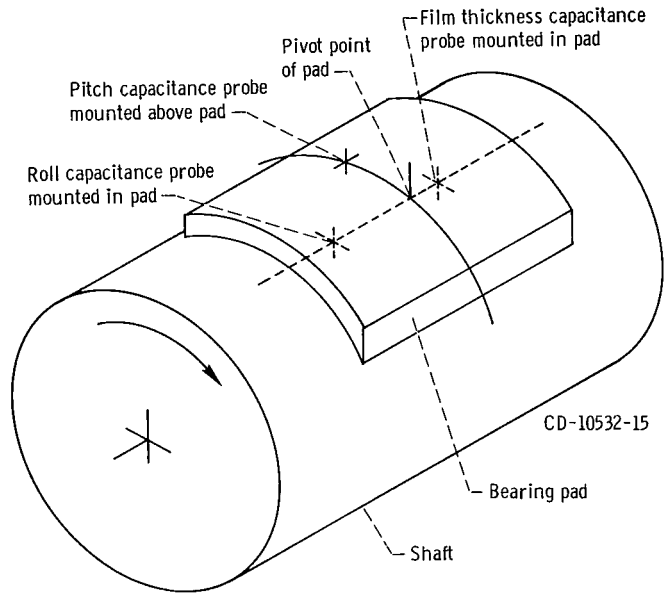

Figure 12. - Location of bearing capacitance probes on typical fully instrumented journal bearing pad.

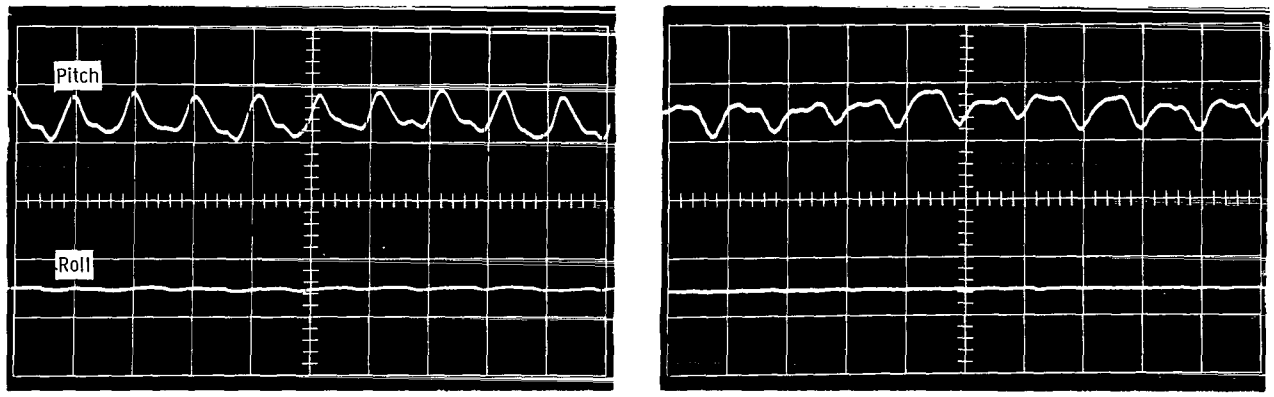

(a) Alternator output, 0 kilowatt electric.

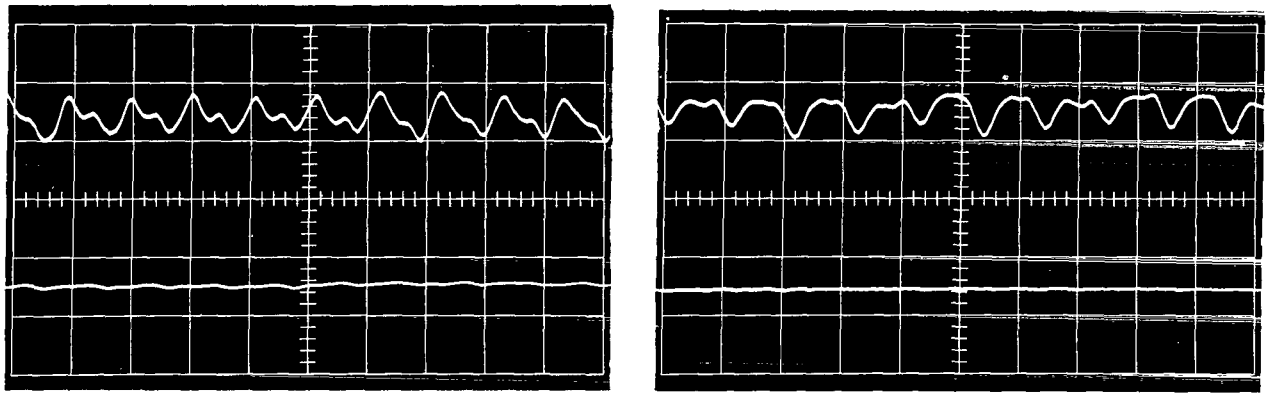

(b) Alternator output, 9 kilowatts electric.

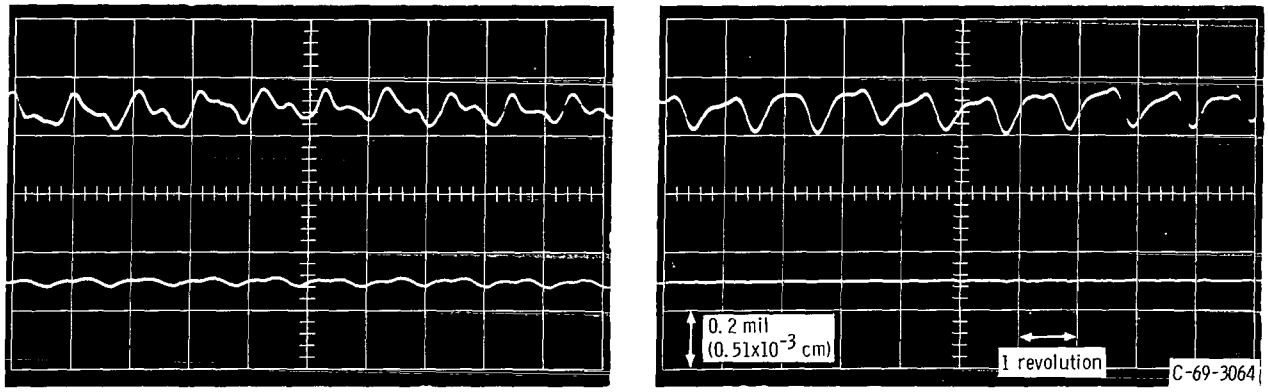

Drive-end pad motions

Anti-drive-end pad motions

(c) Three-phase short circuit.

Figure 13. - Pad roll and pitch motions at various alternator loads. Turbine inlet pressure, 8.45 psia (5.82 N/cm^2); turbine inlet temperature, 1225° F (936 K); alternator speed, 12 000 rpm.

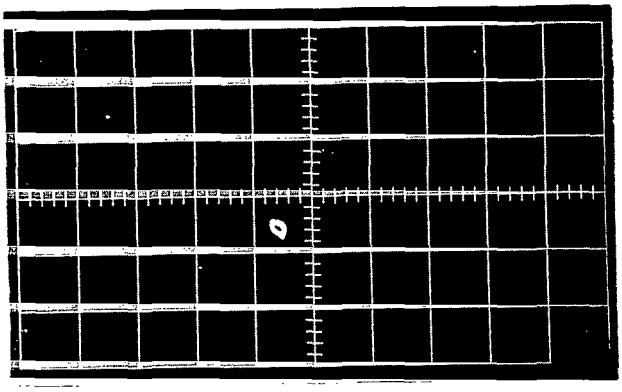

(a) Alternator speed, 9000 rpm.

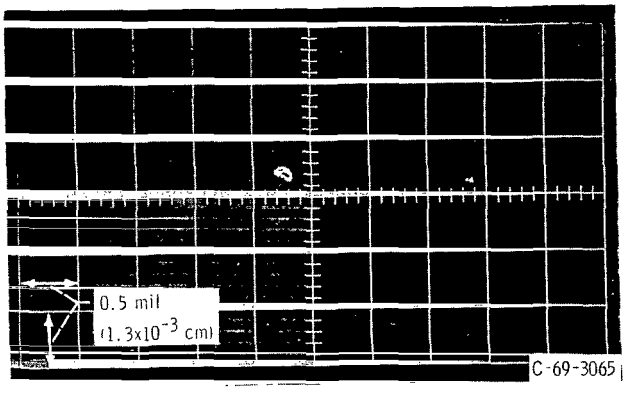

(b) Alternator speed, 7200 rpm.

Figure 14. - Anti-drive-end bearing-journal orbits at 9000- and 7200-rpm resonant points.

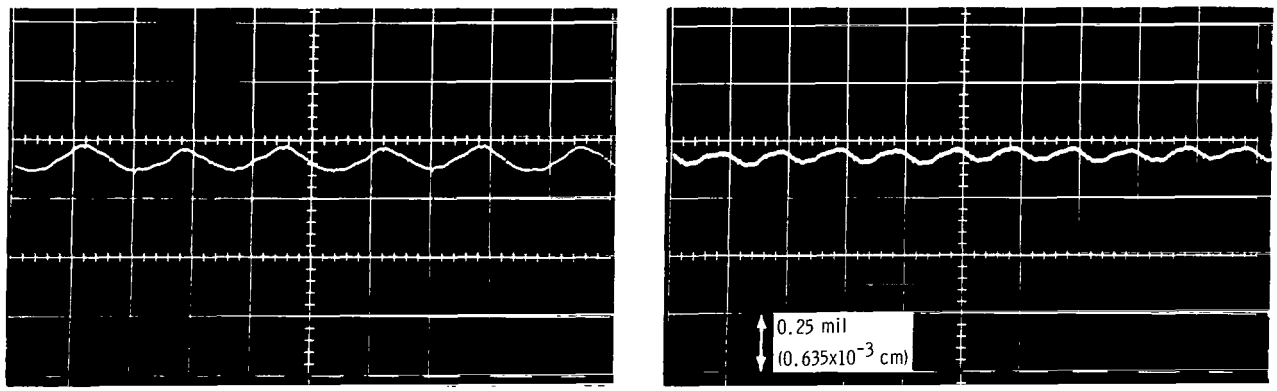

(a) Typical pad film thickness variation at 7200 and 12 000 rpm.

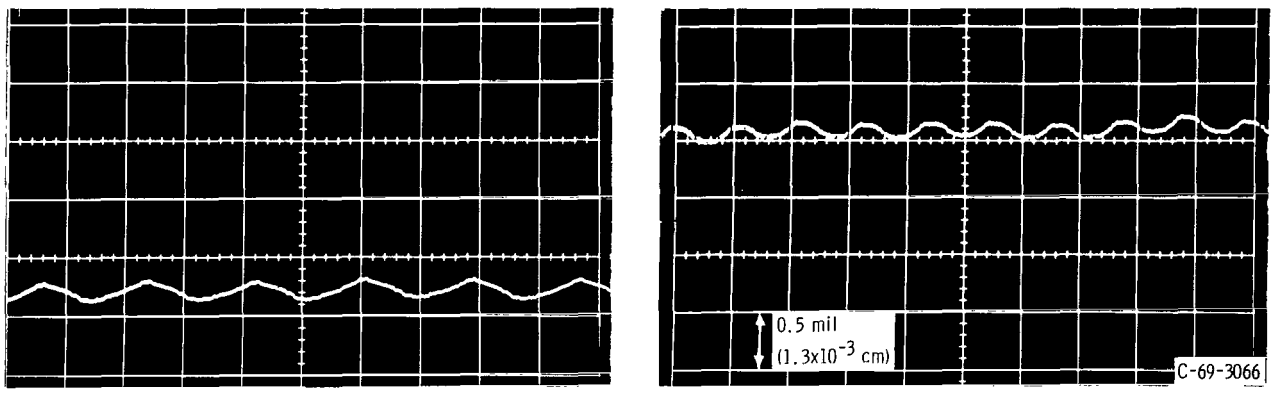

7200 rpm 12 000 rpm

(b) Reverse-thrust-bearing film thickness variation at 7200 and 12 000 rpm.

Figure 15. - Pad film thickness and reverse-thrust-bearing film thickness variation at 7200 rpm (resonance) and at 12 000 rpm (design).

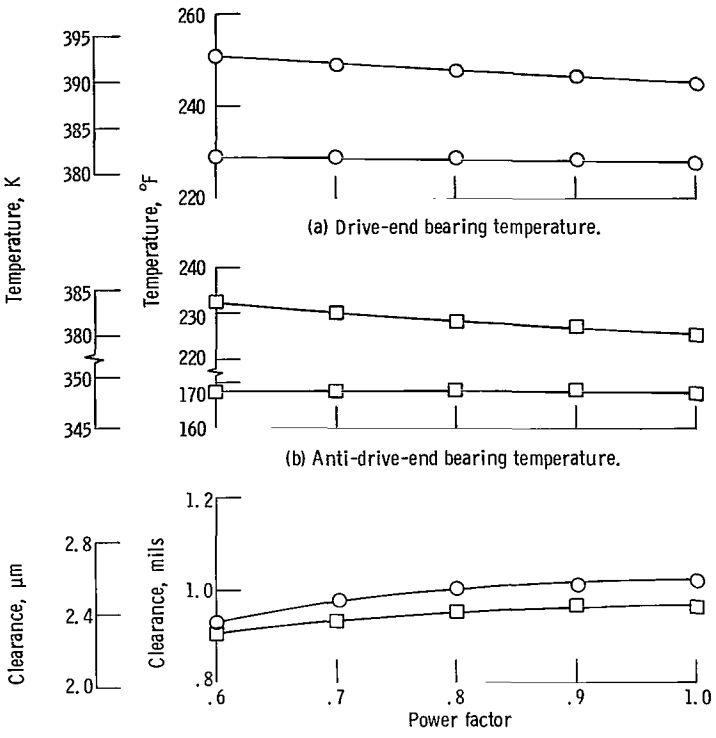

Figure 16. - Effects of power factor on journal clearance and temperature at 9 kilowatts electric and 12 000 rpm.

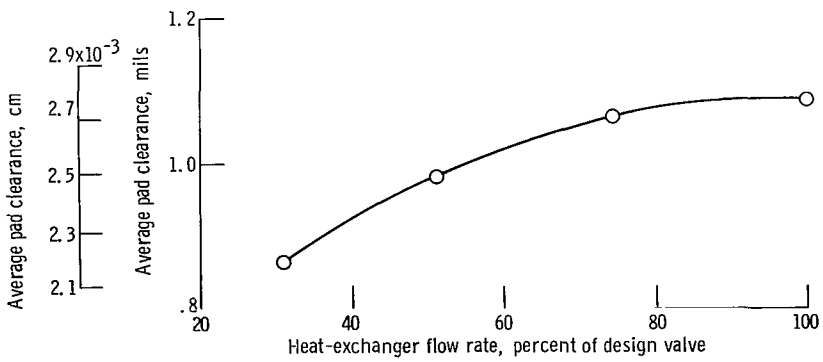

Figure 17. - Effect of liquid coolant flow to journal heat exchangers on drive-end bearing clearance. Turbine inlet pressure, 8.45 psia (5.82 N/cm^2); turbine inlet temperature, 1225° F (936 K); alternator power output, 8.9 kilowatts electric; alternator speed, 12 000 rpm.

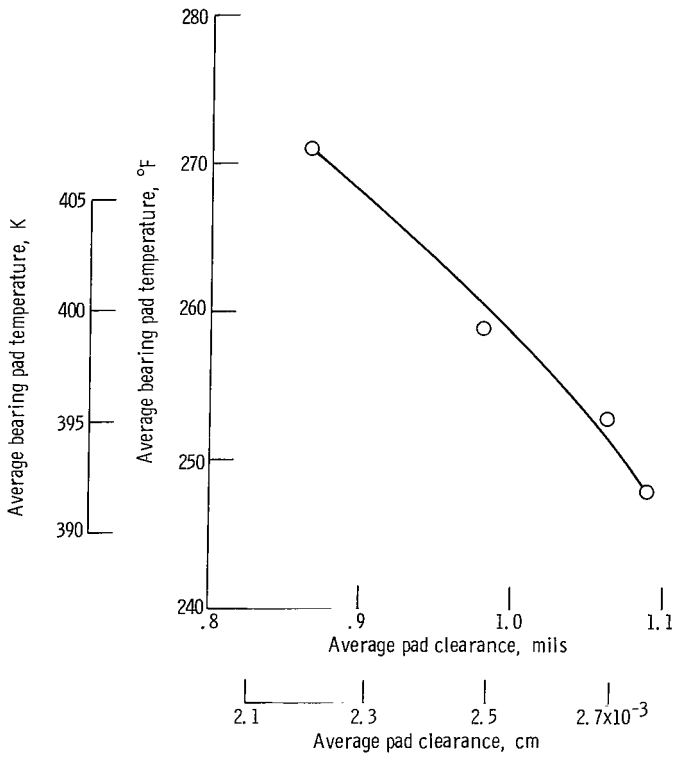

Figure 18. - Effect of pad temperature on drive-end bearing clearance. Turbine inlet pressure, 8.45 psia (5.82 N/cm^2); turbine inlet temperature, 1225° F (936 K); alternator output, 8.9 kilowatts electric; alternator speed, 12 000 rpm.

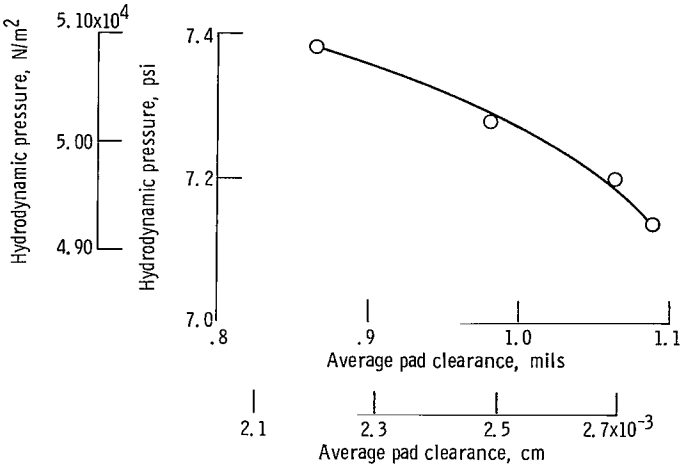

Figure 19. - Effects of journal clearance on hydrodynamic bearing pad pressure (ratio of pivot pressure to cavity pressure) for drive-end journal. Turbine inlet temperature, 1225° F (936 K); turbine inlet pressure, 8.45 psia (5.82 N/cm^2); alternator output, 8.9 kilowatts electric; alternator speed, 12 000 rpm; bearing cavity pressure, 6.36 psi (4.39x10^4 N/m^2).

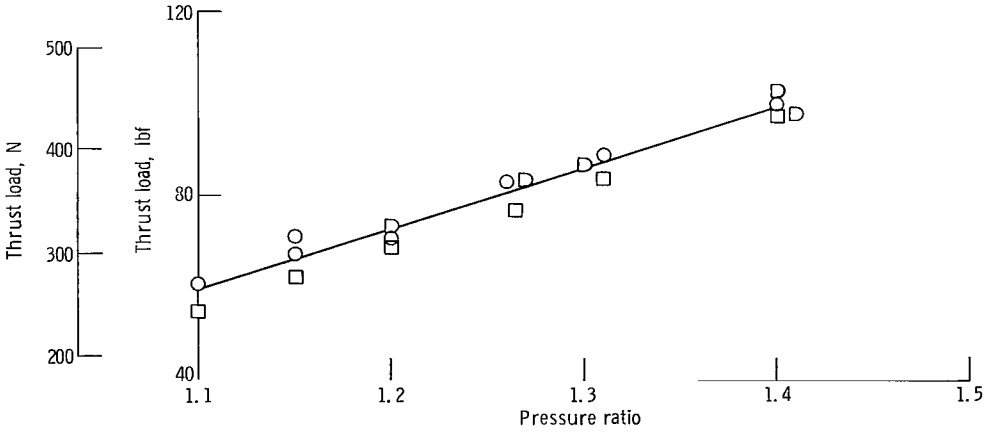

Figure 20. - Effects of pressure ratio on main-thrust-bearing load. Turbine inlet pressure, 8.45 psia (5.82 N/m^2).

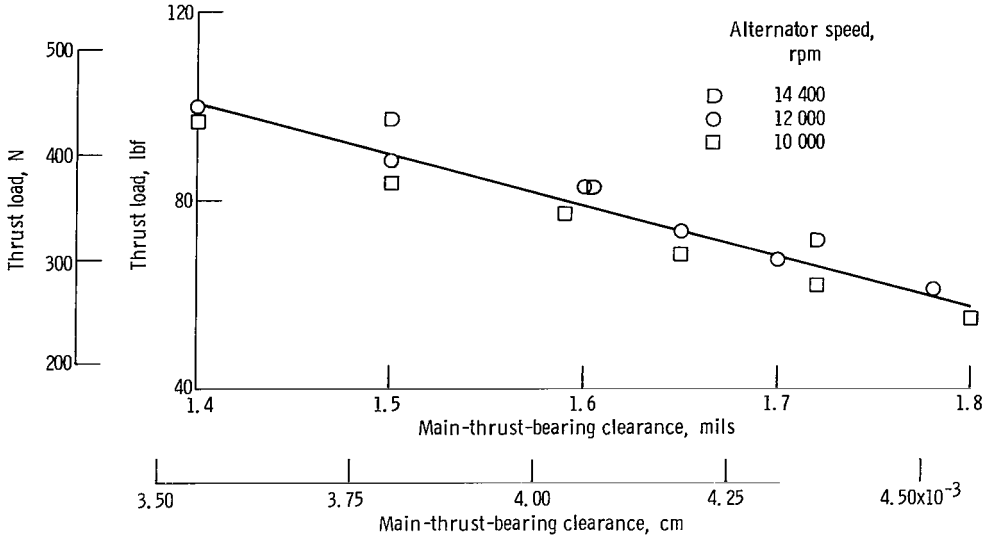

Figure 21. - Effects of thrust load on main-thrust-bearing clearance.

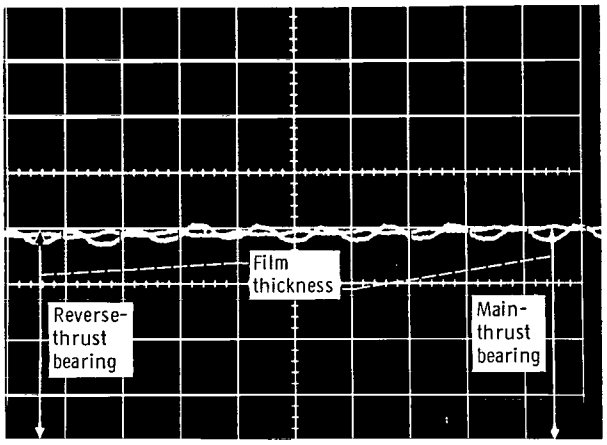

(a) Main thrust load, 60 lbf (256 N); pressure ratio, 1.09.

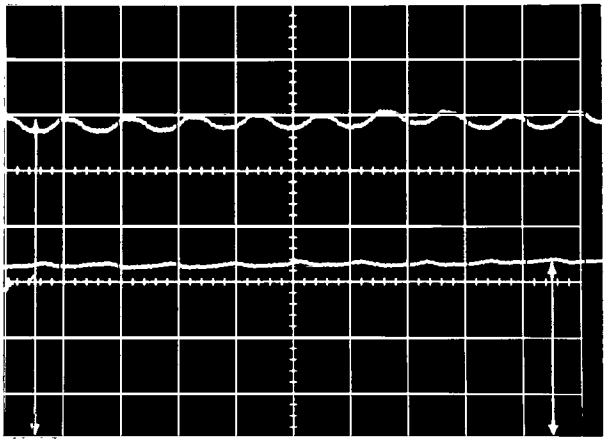

(b) Main thrust load, 85 lbf (378 N); pressure ratio, 1.28.

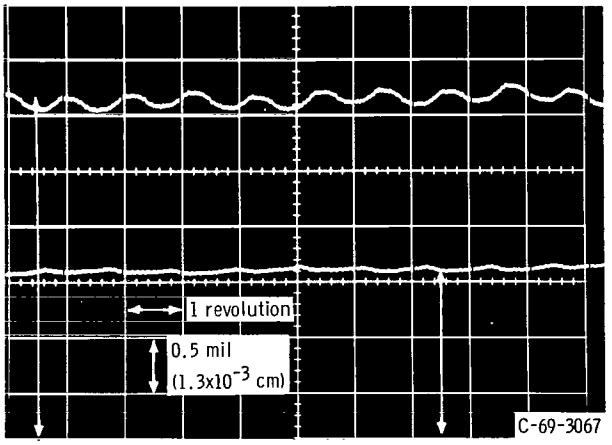

(c) Main thrust load, 90 lbf (400 N); pressure ratio, 1.33.

Figure 22. - Reverse- and main-thrust-bearing film thickness; alternator speed, 12 000 rpm.

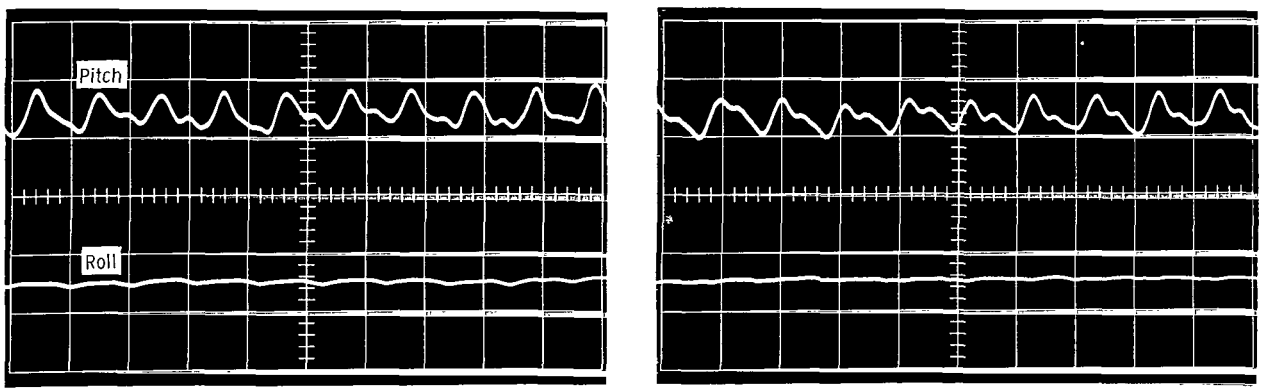

(a) Drive-end pad pitch and roll motions.

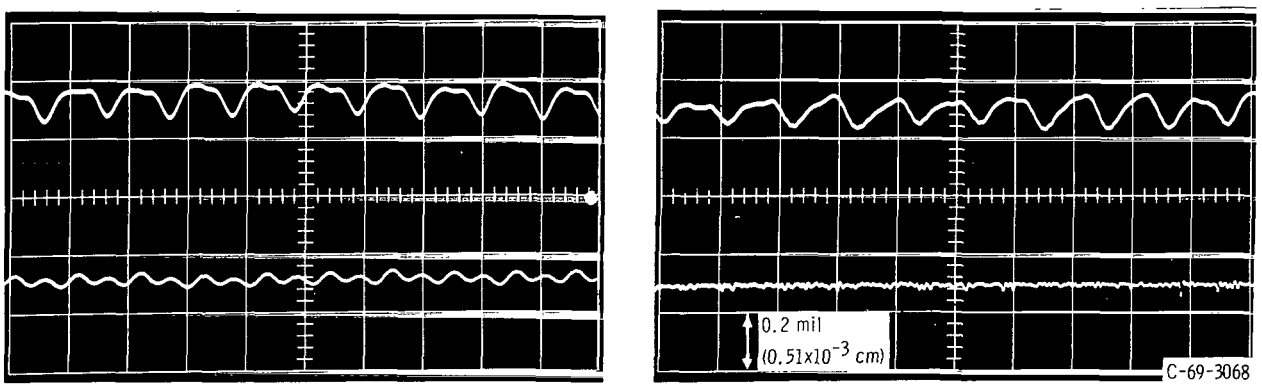

200 Hours

1100 Hours

(b) Anti-drive-end pad pitch and roll motions.

Figure 23. - Pad motions at 200 and 1100 hours of operation. Turbine inlet temperature, 1225° F (936 K); alternator speed, 12 000 rpm; pressure ratio, 1.26. (Roll motion not recorded at 1100 hr because of instrument failure.)

NATIONAL AERONAUTICS AND SPACE ADMINISTRATION
WASHINGTON, D. C. 20546

OFFICIAL BUSINESS

FIRST CLASS MAIL

POSTAGE AND FEES PAID
NATIONAL AERONAUTICS AND
SPACE ADMINISTRATION

POSTMASTER: If Undeliverable (Section 158 Postal Manual) Do Not Return

"The aeronautical and space activities of the United States shall be conducted so as to contribute . . . to the expansion of human knowledge of phenomena in the atmosphere and space. The Administration shall provide for the widest practicable and appropriate dissemination of information concerning its activities and the results thereof."

—NATIONAL AERONAUTICS AND SPACE ACT OF 1958

NASA SCIENTIFIC AND TECHNICAL PUBLICATIONS

TECHNICAL REPORTS: Scientific and technical information considered important, complete, and a lasting contribution to existing knowledge.

TECHNICAL NOTES: Information less broad in scope but nevertheless of importance as a contribution to existing knowledge.

TECHNICAL MEMORANDUMS: Information receiving limited distribution because of preliminary data, security classification, or other reasons.

CONTRACTOR REPORTS: Scientific and technical information generated under a NASA contract or grant and considered an important contribution to existing knowledge.

TECHNICAL TRANSLATIONS: Information published in a foreign language considered to merit NASA distribution in English.

SPECIAL PUBLICATIONS: Information derived from or of value to NASA activities. Publications include conference proceedings, monographs, data compilations, handbooks, sourcebooks, and special bibliographies.

TECHNOLOGY UTILIZATION PUBLICATIONS: Information on technology used by NASA that may be of particular interest in commercial and other non-aerospace applications. Publications include Tech Briefs, Technology Utilization Reports and Notes, and Technology Surveys.

Details on the availability of these publications may be obtained from:

SCIENTIFIC AND TECHNICAL INFORMATION DIVISION

NATIONAL AERONAUTICS AND SPACE ADMINISTRATION

Washington, D.C. 20546